Acylation state of the phosphatidylinositol mannosides from Mycobacterium bovis bacillus Calmette Guérin and ability to induce granuloma and recruit natural killer T cells.

M. Gilleron, C. Ronet, M. Mempel, B. Monsarrat, Gabriel Gachelin, G. Puzo

THE JOURNAL OF BIOLOGICAL CHEMISTRY
Vol. 276, No. 37, Issue of September 14, pp. 34896–34904, 2001
Printed in U.S.A.

Acylation State of the Phosphatidylinositol Mannosides from *Mycobacterium bovis* Bacillus Calmette Guérin and Ability to Induce Granuloma and Recruit Natural Killer T Cells*

Received for publication, May 1, 2001, and in revised form, June 15, 2001
Published, JBC Papers in Press, July 5, 2001, DOI 10.1074/jbc.M103908200

Martine Gilleron‡§, Catherine Ronet¶, Martin Mempel¶, Bernard Monsarrat‡, Gabriel Gachelin¶, and Germain Puzo‡

From the ‡Institut de Pharmacologie et de Biologie Structurale du CNRS, 205 Route de Narbonne, 31077 Toulouse Cedex and ¶Unité de Biologie Moléculaire du Gène, Institut Pasteur, 25 Rue du Dr. Roux, 75284 Paris Cedex 15, France

Previous studies have found that, when injected into mice, glycolipidic fractions of mycobacterial cell walls containing phosphatidylinositol mannosides (PIM) induced a granuloma and recruitment of Natural Killer T cells in the lesions. The dimannoside (PIM_2) and the hexamannoside (PIM_6) PIM were isolated from *Mycobacterium bovis* bacillus Calmette Guérin and shown to act alike, but the activity was found to be dependent on the presence of the lipidic part. The chemical structure of PIM was then re-evaluated, focusing on the characterization of their lipidic part, defining mono- to tetra-acylated PIM_2. The structure of these acyl forms was elucidated using a sophisticated combination of chemical degradations and analytical tools including electrospray ionization/mass spectrometry, electrospray ionization/mass spectrometry/mass spectrometry, and two-dimensional NMR. Finally, the acyl forms were purified by hydrophobic interaction chromatography and tested for their capacity to induce the granuloma and Natural Killer T cell recruitment. We found that there is an absolute requirement for the molecules to possess at least one fatty acyl chain, but the number, location, and size of the acyl chains was without effect. Moreover, increasing the complexity of the carbohydrate moiety did not lead to significant differences in the biological responses.

Phosphatidyl-*myo*-inositol mannosides (PIM)[1,2] constitute a group of phospholipids found in the cell wall and the cytoplasmic membrane of mycobacteria along with cardiolipid, phosphatidylethanolamine, and phosphatidylinositol. Known from the 1940s and fully described by Ballou and colleagues (1) in the 1960s, they were shown to consist of phosphatidyl-*myo*-inositol di-, tri-, tetra-, and pentamannosides (PIM_2 to PIM_5). These authors showed unequivocally that in PIM_2 the mannosyl units were glycosidically attached at positions 2 and 6 of the *myo-Ins* ring (2) and that for the more glycosylated forms, chain elongation occurred on the mannose present at position 6 (3). Recently, PIM from *Mycobacterium smegmatis* were reanalyzed in their deacylated form (4). They were shown to have a structure based on that defined by Ballou *et al.* (1) but containing six mannosyl residues (PIM_6). The structure of the glycosidic part of PIM_6 is now unambiguously established and corresponds to Man*p*α-1→(2-Man*p*α-1)$_2$→(6-Man*p*α-1)$_2$→ linked to position 6 of the *myo-Ins* ring beside the mannosyl residue present at position 2. This structure was confirmed by an NMR spectroscopy strategy applied to deacylated PIM_6 (5).

Concerning the lipidic part of the PIM, the situation is still unclear, although the presence of multiacylated forms of PIM was already reported in 1960s by several authors (6–9) working on different mycobacterial strains. More recently, in a chromatographic and fatty acid quantitation study of mycobacterial lipoglycans, Leopold and Fisher (10) also inferred the existence of multiacylated forms of PIM. However, the sites of attachment of the acyl groups were not established. Re-evaluating the multiacylated nature of *Mycobacterium tuberculosis* and *Mycobacterium leprae* PIM using FAB-MS analysis, Brennan's group (11) presented evidence for tri-acylated PIM, assuming an extra fatty acyl group on the C-6 of one of the Man*p* residue beside the fatty acids already localized on the C-1 and C-2 of the glycerol. Our data derived from an NMR study of a tetra-acylated form of PIM_2 (Ac_4PIM_2) purified from *Mycobacterium bovis* BCG clearly inferred the previously described positions and demonstrated the fourth acylation site as the C-3 of the *myo*-Ins (12).

Recently, PIM received a renewed interest due to the fact that PIM_2 constitute the anchor motif of two important constituents of the mycobacterial cell walls, namely lipomannans (LM) and lipoarabinomannans (LAM). LAM, ubiquitous in the *Mycobacterium* genus, exhibit a wide spectrum of immunoregulatory effects (for reviews see Refs. 13–15). It is now clearly established that most of these effects are abolished by alkaline hydrolysis, highlighting the importance of the lipidic part of the anchor. Moreover, PIM_6 as well as ManLAM from *M. leprae* and *M. tuberculosis* Erdman strain are recognized by human $CD4^-CD8^-$ α/β T cells in the context of a presentation by CD1b-expressing antigen-presenting cells (16). The high affin-

* The costs of publication of this article were defrayed in part by the payment of page charges. This article must therefore be hereby marked "*advertisement*" in accordance with 18 U.S.C. Section 1734 solely to indicate this fact.

§ To whom correspondence should be addressed. Tel.: 33 5 61 17 55 04; Fax: 33 5 61 17 59 94; E-mail: gilleron@ipbs.fr.

[1] The abbreviations used are: PIM, phosphatidyl-*myo*-inositol mannosides; PIM_2, PIM_3, PIM_4, PIM_5, PIM_6, phosphatidyl-*myo*-inositol di-, tri-, tetra-, penta-, and hexamannosides; BCG, bacillus Calmette Guérin; CDR, complementary determining region; ESI-MS, electrospray ionization/mass spectrometry; FAB-MS, fast atom bombardment/mass spectrometry; GC/MS, gas chromatography/mass spectrometry; HMBC, heteronuclear multiple bound correlation spectroscopy; HMQC, heteronuclear multiple quantum correlation spectroscopy; HOHAHA, homonuclear Hartmann-Hahn spectroscopy; LAM, lipoarabinomannans; LM, lipomannans; ManLAM, LAM with mannosyl extensions; NK T, Natural Killer T cells; QMA, quaternary methyl ammonium; TCR, T cell antigen receptor; Man, mannosyl unit; *myo*-Ins, *myo*-inositol; Gro, glycerol; *p*, pyranosyl; PCR, polymerase chain reaction; PBS, phosphate-buffered saline; PI, phosphatidylinositol.

[2] PIM is used here to describe the global family of PIM that carries one to four fatty acids. In Ac_XPIM_Y, the number of acyl groups cited (X) refers to the total number, including those attached to the glycerol, *e.g.* Ac_4PIM_2 corresponds to the tetra-acylated form of PIM_2.

ity interaction of CD1b molecules with the PIM_2 acyl side chains was then established (17). The phosphatidylinositol moiety plays a central role in the process of PIM and ManLAM binding to CD1b proteins. In the mouse, *CD1a, -b*, and *-c* genes are missing. The murine *CD1d* gene is homologous to the *CD1d* gene in man (18). This CD1d molecule restricts $CD4^+$ or DN T cells (NK T cells) using a distinctive TCR characterized by an invariant α chain (19–21). The crystal structure of the mouse CD1d1 molecule showed a hydrophobic binding site (22), and cellular glycosylphosphatidylinositol was proposed as a major natural ligand (23). Due to the homology between CD1a, -b, -c, and -d molecules, it has been hypothesized that mouse CD1d may bind mycobacterial glycolipids. In this respect, a recent study reported that granuloma formation in response to a crude fraction containing PIM from H37Rv *M. tuberculosis* was dependent upon CD1d-restricted T cells (20). However, no reports have mentioned PIM presentation by CD1d molecules, and the respective roles of the lipidic and carbohydrate moieties in the PIM-induced response was not established.

In this study, the chemical structure of PIM isolated from *M. bovis* BCG was evaluated, focusing on the characterization of the lipidic part of the PIM, thus defining the notion of "acyl forms." The structure of these acyl forms was elucidated using sophisticated analytical tools such as ESI-MS, ESI-MS/MS, and two-dimensional NMR. Finally, these acyl forms were purified and used in a bioassay aimed at determining the extent of inflammation they caused and the recruitment of NK T cells into the granulomatous lesions they induced.

EXPERIMENTAL PROCEDURES

Mice—C57BL/6 mice were 6–8-week-old and obtained from IFFA-Credo (L'Arbresle, France). Mice were injected subcutaneously with 50 μg of each molecule and adsorbed onto 12.5 μl of a neutral carrier (Alu-Gel-S, Serva) in a total volume of 0.1 ml. The cellular infiltrate at the site of the injection was excised 7 days after the injection and either fixed for histological analysis or used for mRNA characterization.

RNA Extraction and cDNA Synthesis—Total RNA was isolated by using the Trizol technique (Life Technologies, Inc.). cDNA was synthesized from 10 μg of total RNA, using a $(dT)_{17}$ primer, 25 units of RNasin (Promega Corp., Madison, WI), and 10 units of avian myeloblastosis virus-reverse transcriptase (Roche Molecular Biochemicals) in the provided buffer.

mRNA Quantification, PCR Procedure, and Immunoscope Analysis—HGPRT-standardized amounts of cDNA solution were PCR-amplified using Vα14- and Cα-specific primers (20). PCR products were subjected to primer extension using an internal, fluorescently labeled Cα-specific primer (to approach the total usage of $V\alpha14^+$ segments) or a Jα281-specific primer (to generate only signals due to the NK T-specific rearranged Vα14-Jα281 TCR α chain) (20). Run-off products were analyzed on an automatic sequencer. The size and the intensity of each band were recorded and analyzed using the Immunoscope software (Applied Biosystems, Inc.). Typically, a random usage of all rearranged Vα14 α chains is depicted as a series of peaks corresponding to in-frame mRNA, each corresponding to a define length of the CDR3 region. A selected usage of a rearranged chain appears as a peak that distorts the abovementioned gaussian-like distribution; the NK T-specific Vα14-Jα281 TCR α chain appears as a peak with a CDR3 length of 10 amino acids (20).

PIM Extraction—The PIM-containing lipidic extract was obtained during the *M. bovis* BCG phenolic glycolipids purification (24). Briefly, 1300 g of *M. bovis* BCG cells were suspended in chloroform/methanol (1:1, v/v) and filtered. The cells were suspended four times in the same way. The whole lipid extract was concentrated and partitioned between water and chloroform. The chloroform phase was evaporated, and the residue was suspended in hot acetone and then allowed to deposit overnight at 4 °C. The suspension was then centrifuged at 4 °C for 20 min (3000 × *g*) yielding 40 g of acetone-insoluble phospholipids-containing lipid extract. 7 g of this extract was applied to a QMA-Spherosil M (BioSepra SA, Villeneuve-la-Garenne, France) column (3.0 × 20 cm) that was first irrigated with 300 ml of chloroform, chloroform/methanol (1:1, v/v), methanol in order to elute neutral compounds. Phospholipids were eluted using ammonium acetate containing organic solvents. Indeed, 0.1 M ammonium acetate in chloroform/methanol (1:2, v/v) (fraction A) allowed elution of 750 mg of phospholipids (phosphatidyl-*myo*-inositol dimannosides (PIM_2) essentially); 0.2 M ammonium acetate in chloroform/methanol (1:2, v/v) (fraction B) was subdivided into two fractions as follows: the 1st volumes allowed elution of 440 mg of phospholipids (cardiolipids essentially) and the next ones allowed elution 160 mg of phospholipids (mixture of phosphatidyl-*myo*-inositol di-(PIM_2) and hexa- (PIM_6) mannosides), and finally, 0.2 M ammonium acetate in methanol (fraction C) allowed elution of 55 mg of phospholipids (PIM_6 essentially). Repeated lyophilizations were necessary to eliminate ammonium acetate salts.

Purification of the PIM Acyl Forms—170 mg of the fraction A containing mainly PIM_2 were first flash-chromatographed on a silicic acid column (2.5 × 30 cm) (KG60, 230–400 mesh, Merck) using chloroform/methanol/water, 90:10:1; 80:20:1; 70:30:2; 70:30:4; 60:35:6 successively as eluents. PIM_2Ac_4 was recovered in the 70:30:2 fraction (12). Fractions corresponding to 70:30:4 (60 mg) and 60:35:6 (70 mg) elutions were independently re-chromatographed by isocratic silicic flash chromatography (2 × 23 cm columns) unsuccessfully in order to purify more polar PIM_2. Then, 20 mg of the fraction A were then loaded in 0.1 M ammonium acetate solution containing 25% (v/v) propanol-1 to octyl-Sepharose CL-4B (Amersham Pharmacia Biotech) column (20 × 1.5 cm) pre-equilibrated with the same buffer. The column was first eluted with 50 ml of equilibration buffer and then with a linear propanol-1 gradient from 25 to 50% (v/v) (125 ml each) in 0.1 M ammonium acetate solution at a flow rate of 5 ml/h. The fractions were collected each 15 min. 20 μl of each fraction was dried and submitted to acidic hydrolysis (100 μl trifluoroacetic acid 2 M, 2 h, 110 °C). The hydrolysates were dried, reconstituted in water, and then analyzed by high pH anion exchange chromatography for mannose content.

Purification was checked by TLC, on aluminum backed plates of silica gel (Alugram Sil G, Macherey-Nagel, Duren, Germany) using as migration solvent chloroform/methanol/water, 60:35:6 (v/v/v). A sulfuric anthron spray and a Dittmer-Lester spray were used to detect carbohydrates containing lipids and phosphorus-containing lipids, respectively.

Acetolysis Procedure—200 μg of PIM were treated with 200 μl of anhydrous acetic acid/acetic anhydride, 1:1, v/v at 110 °C for 12 h. The reaction mixture was dried under stream of nitrogen and was submitted to acetylation. The mixture was dissolved in acetic anhydride/anhydrous pyridine, 1:1, v/v at 80 °C for 2 h. The reaction mixture was dried under stream of nitrogen. 200 μl of chloroform/methanol, 9:1, v/v was added, and negative mass spectrum was recorded using about 100 μl of mixture. The remaining mixture was dried and then dissolved in 100 μl of 0.1 M ammonium acetate in chloroform/methanol, 9:1, v/v, and positive mass spectrum was recorded. The same protocol was applied using perdeutero-acetylated reactives in order to deduce the number of acetates present after peracetylation.

Electrospray Mass Spectrometry (ESI-MS)—The phospholipids were dissolved in chloroform/methanol/water (60:35:8, v/v/v) in order to be analyzed in ESI-MS. ESI-MS analyses were carried out on a Finnigan Mat TSQ 700 triple quadrupole mass spectrometer (Finnigan Mat, San Diego, CA) system. The negative ESI mode (spray potential 3.8 kV, temperature of heated capillary 140 °C) and positive ESI mode (spray potential 4.8 kV) were used. The mass spectra were obtained by direct infusion using a syringe pump (Harvard Apparatus) at a flow rate of 4 μl min^{-1}. Full scan spectra were acquired in the ion peak centroid or profile modes over the mass/charge range of 200–3000 at 2.0–3.0 s. Tandem mass spectrometry (MS/MS) experiments were based by conducting collision-induced dissociation occurring in the radio-frequency-only collision cell of the triple quadrupole at a collision energy of 40–80 eV. Argon was used as collision gas in the range of 1.5–2.5 mtorr. At least 15 scans were accumulated and averaged. Data analysis was controlled by a DEC α 500 data system.

NMR Spectroscopy—NMR spectra were recorded on a Bruker DMX-500 spectrometer equipped with an Aspect X32 computer. PIM samples were dissolved in $CDCl_3$ (99.96% purity)/CD_3OD (99.8% purity)/D_2O (99.97% purity), 70:30:2, v/v/v and analyzed at 20 °C. Deuterated solvents were purchased from Eurisotop, Saint Aubin, France. Samples were analyzed in a 200 × 5 mm 535-PP NMR tubes. Chemical shifts are expressed in ppm downfield from the signal of $CDCl_3$ (δ_H/trimethylsilyl 7.27 and δ_C/trimethylsilyl 77.7).

All two-dimensional NMR data sets were recorded without sample spinning, and data were acquired in the phase-sensitive mode using the time-proportional phase increment (25). Two-dimensional homonuclear Hartmann-Hahn (HOHAHA) spectrum was recorded using MLEV-17 mixing sequence of 30 ms (26). ^1H-^{13}C correlation spectra were recorded in the proton-detected mode with a Bruker 5-mm ^1H-broadband tunable probe with reversal geometry. The ^1H-^{13}C and ^1H-^{31}P single-bond cor-

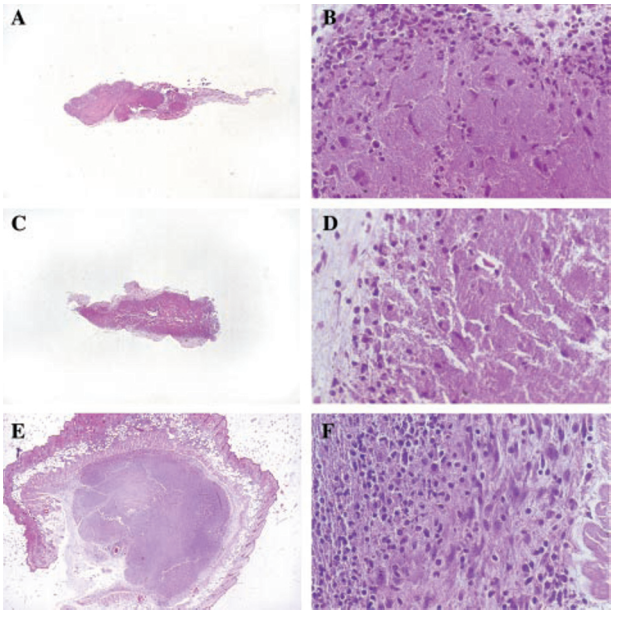

FIG. 1. **Structure of the granuloma generated by injecting phosphatidylinositol mannosides.** The granuloma were excised 7 days following the injection, fixed with formalin, sectioned, and stained using hematoxylin-eosin. *Left panels,* magnification × 20. *Right panels,* magnification × 400. *A* and *B,* injection of PBS-Alum. *C* and *D,* injection of deacylated fraction A-Alum. *E* and *F,* injection of the fraction A-Alum.

relation spectra (HMQC) were obtained according Bax's pulse sequence (27). The GARP sequence (28) at the carbon or phosphorus frequency was used as a composite pulse decoupling during acquisition. Multiple-bond ^{1}H-^{13}C correlation spectra (HMBC) (29) were processed in the magnitude mode. The pulse sequence used for ^{1}H-detected heteronuclear relayed spectra (HMQC-HOHAHA) was that of Lerner and Bax (30).

RESULTS

Isolation of PIM Acyl Forms Inducing Granuloma—From previous data (31), phosphatidyl-*myo*-inositol mannosides (PIM) are known to be found in the acetone-insoluble fraction of the chloroform/methanol (1:1, v/v) mycobacterial extract. The contaminating neutral compounds were eliminated by QMA anion exchange chromatography, irrigated with neutral eluents (chloroform, followed by chloroform/methanol, 1:1, v/v and then by methanol). Then, phospholipids were eluted with ammonium acetate-containing organic solvents resulting in three fractions, namely A–C. Each fraction was adsorbed onto alum and injected subcutaneously to C57BL/6 mice. Seven days after the injection, the cell infiltrates were excised, sectioned, and stained. The three fractions generated a highly organized and large granuloma with a central core of neutrophils surrounded by a densely organized rim of macrophages, lymphocytes, and fibroblasts (Fig. 1, *E* and *F*), mimicking the granuloma observed during murine tuberculosis. By contrast, a minor inflammatory reaction was evidenced in PBS-injected (control mice) (Fig. 1, *A* and *B*) or deacylated PIM-injected mice (Fig. 1, *C* and *D*). In this case, the lesions were found to predominantly contain a disordered array of macrophages and neutrophils with few lymphocytes. This points to the absolute requirement for the lipidic moiety of PIM to cause a granulomatous lesion.

In order to characterize the PIM composition of the different fractions, the fractions A–C were analyzed by ESI-MS in negative mode. The attribution of the deprotonated molecular ions $(M - H)^-$ (Fig. 2) was based on the predominant fatty acids as deduced from GC/MS analysis (not shown), *i.e.* palmitic (C_{16}), tuberculostearic (C_{19}), and stearic (C_{18}) acids. ESI-MS mass

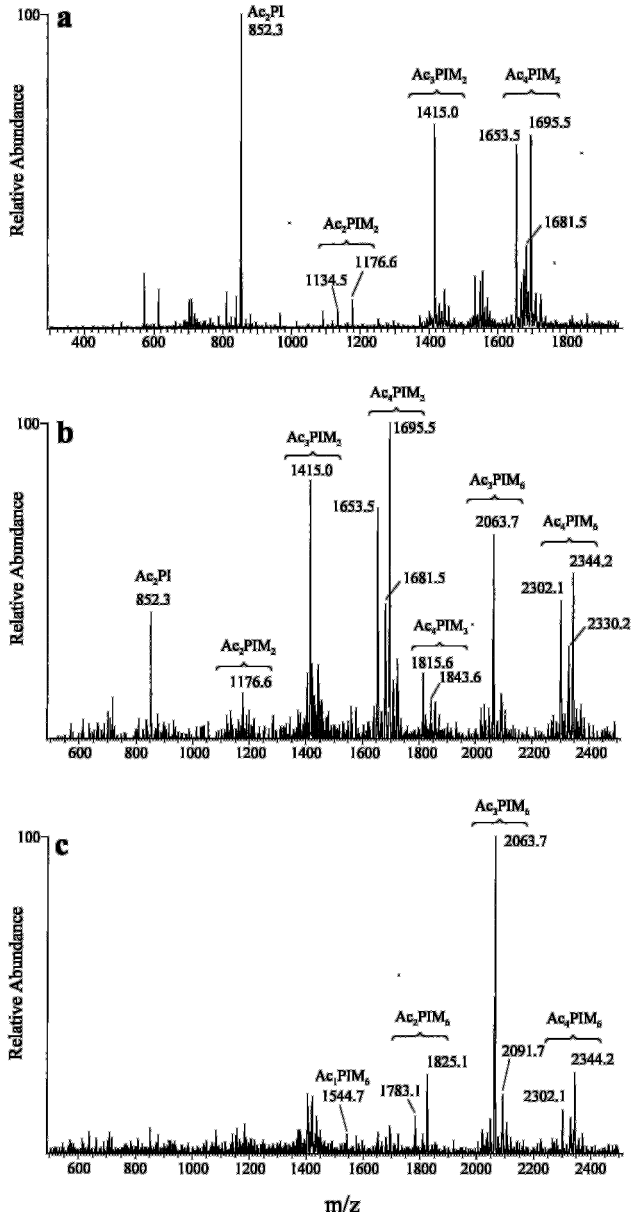

FIG. 2. **Negative ESI mass spectra of the A-C fractions (*a–c*).**

spectrum of fraction A predominantly showed ions corresponding to Ac_3- (m/z 1415.0) and Ac_4- (m/z 1653.5, 1681.5 and 1695.5) PIM_2 in addition to the diacyl form of phosphatidylinositol (Ac_2PI at m/z 852.3) (Fig. 2*a*). Fraction B mass spectrum (Fig. 2*b*) appeared more complex showing predominantly the previously described Ac_3- and Ac_4PIM_2 and also Ac_3- (m/z 2063.7) and Ac_4- (m/z 2302.1, 2330.2, and 2344.2) PIM_6. Finally, the mass spectrum of fraction C (Fig. 2*c*) was dominated by one peak at m/z 2063.7 assigned to $(M - H)^-$ of Ac_3PIM_6, beside the other acyl forms of PIM_6. In summary, tri- and tetra-acylated forms of PIM_2 and PIM_6 appeared to be the most abundant PIM acyl forms of *M. bovis* BCG, and they may be responsible for the granuloma formation.

Purification of the PIM Acyl Forms—The first attempt to go further in the separation of the different PIM acyl forms consisted of using silicic phase flash-chromatography with chloroform/methanol/water in different proportions as eluents. By using this strategy, Ac_4PIM_2 was purified from fraction A with a chloroform/methanol/water, 70:30:2, v/v/v eluent (12). The fractionation of the more polar PIM_2 and PIM_6 was unsuccessful using successive isocratic flash chromatographies. An alter-

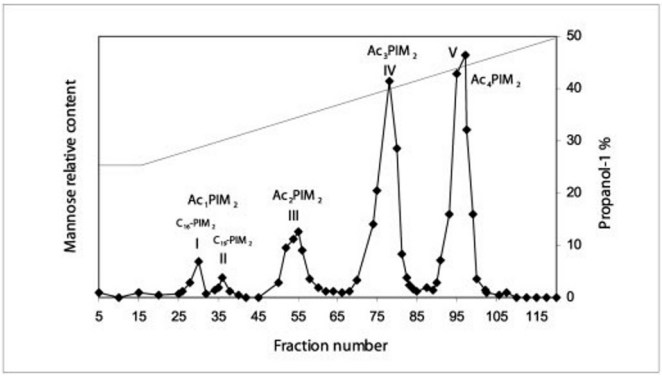

FIG. 3. **Octyl-Sepharose chromatography of the PIM_2-containing fraction A.** The column was eluted with a propanol-1 linear gradient (25–50% (v/v)) in 0.1 M ammonium acetate. Fractions were analyzed by high pH anion exchange chromatography for their mannose content.

native approach was developed, using hydrophobic interaction chromatography on an octyl-Sepharose column, with propanol-1 as eluent. Fig. 3 shows the purification of PIM_2 acyl forms issued from fraction A. The different acyl forms were eluted at propanol-1 concentrations ranging from 25 to 50% and separated into 5 sub-fractions according to the mannose content profile. Each sub-fraction (I–V) was collected and analyzed by ESI-MS and NMR.

Strategy for the Structural Elucidation of the Acyl Forms, the Example of Ac_3PIM_2—The negative ESI mass spectrum of fraction IV is dominated by the signal at m/z 1414.2 (Fig. 4*c*), beside peaks at m/z 1442.2 and m/z 1456.2 assigned to deprotonated molecular ions of tri-acylated forms of PIM_2 (Ac_3PIM_2). Indeed, the most abundant $(M - H)^-$ ions at m/z 1414.2 (77%) characterized Ac_3PIM_2 esterified by $2C_{16}$,$1C_{19}$, whereas the ions at m/z 1442.2 (14%) and 1456.2 (9%) corresponded to PIM_2 esterified by $1C_{16}$,$1C_{18}$,$1C_{19}$ and $1C_{16}$,$2C_{19}$, respectively.

The acylation sites on PIM were determined previously to be at both positions of the Gro, the C-3 of the *myo*-Ins unit and the C-6 of the Man*p* unit linked to C-2 of the *myo*-Ins thanks to an NMR strategy based on two-dimensional ^1H-^{31}P and ^1H-^{13}C experiments applied on the tetra-acylated form of PIM_2 (Ac_4PIM_2) (12). The NMR strategy we applied on each acyl form is presented briefly below. From the ^1H-^{31}P HMQC experiment, the prochiral H-3 and H-3′ Gro protons and the *myo*-Ins H-1 were easily assigned. Then, the remaining *myo-Ins* and Gro protons were observed on the two-dimensional ^1H-^{31}P HMQC-HOHAHA spectrum (Fig. 5) and were assigned from their multiplicity and chemical shifts (32) and with the help of the ^1H-^1H HOHAHA spectrum. The different chemical shifts typified the presence or absence of an acyl appendage. For example, a di-acyl-Gro could be evidenced by an H-2 around 5.10 ppm (and H-1 around 4.00/4.25 ppm) (32) and a lyso-Gro should then be assigned by an H-2 around 3.75 ppm and H-1 around 3.95 ppm. These attributions were then supported by the downfield resonance of the lyso-Gro ^{31}P resonance compared with that of di-acyl-Gro ^{31}P. Likewise, the downfield shift of the *myo*-Ins H-3 of about 1 ppm signed a C-3 acyl appendage. The fourth position of acylation, the C-6 of the Man*p*, was checked with the ^1H-^{13}C HMBC spectrum, which implied the complete determination of ^1H and ^{13}C chemical shifts achieved by ^1H-^1H HOHAHA and ^1H-^{13}C HMQC analysis. When this position is acylated, the H6/H6′ was deshielded from 3.47/3.64 to 3.95/4.07 ppm.

This analytical approach applied to Ac_3PIM_2 (Fig. 5*c*) revealed that the major acyl form corresponded to PIM with two fatty acids on the Gro and one fatty acid on the Man*p* unit. This was definitively demonstrated from the ^1H-^{13}C HMQC spectrum, by the chemical shifts of the H-2 (4.98 ppm) and C-2 (70.6 ppm) of Gro and of the H-6/H-6′ (4.07/3.95 ppm) and C-6 (63.6 ppm) of Man*p*. Beside this species, another one was observed in less quantity. Indeed, ^1H-^{13}C HMQC and ^1H-^1H HOHAHA highlighted the presence of an acylated ($\delta_{H\text{-}3}$ 4.55) *myo*-Ins and of a mono-acyl Gro with the acyl appendage present in position 2 as evidenced by the H-2 at δ 4.80.

The nature of the fatty acids esterifying the different sites was investigated by mass spectrometry using two different approaches. The first consisted in obtaining fragment ions produced by ESI-MS/MS from each pseudo-molecular ion of the native molecule (Fig. 6*a*). Concerning Ac_3PIM_2, Fig. 6*b* shows the MS/MS spectrum obtained from the precursor ions at m/z 1414.2 ($2C_{16}/C_{19}$ PIM_2). This spectrum is dominated by peaks at m/z 297.7 and 255.6 assigned to C_{19} and C_{16} carboxylate fatty acids, respectively. In addition, in the high mass range loss of C_{16} gives the fragment ions at m/z 1158.5 which in turn led to the fragment ions m/z 860.0 by loss of C_{19}. More interesting are the fragment ions C at m/z 803.9 highlighting a C_{16} acyl appendage on the C-6 of the Man*p* residue. Moreover, this spectrum shows fragment ions at m/z 433.4 corresponding to mono-C_{19} Gro and at m/z 153.2 (not shown) corresponding to deacylated Gro. So, ESI-MS/MS fragmentations did not appear suitable in order to establish accurately the structure of the fatty acid located on the glycerol moiety. Moreover, in the case of Ac_4 forms, C ions were unable to discriminate between acyl appendages located on the Man*p* and the *myo*-Ins.

A second approach was then developed, consisting in ESI-MS analysis of the acetolysis reaction products of each PIM_2 species. Acetolysis cleaves the phosphoglycerol linkage without altering the fatty acid esters, leading to two entities as follows: the dimannosyl-inositol phosphate moiety (Man_2-Ins-P) (I, II) and the acyl-glycerol residue (III) (Fig. 7*a*). The dimannosyl-inositol phosphate moiety was observed in negative mode as $[M - H]^-$ ions I and II, and the acyl-glycerol residue was analyzed in positive mode in the presence of ammonium acetate as $[M + NH_4]^+$ ions III. The acetolysis reaction produces two populations of dimannosyl-inositol phosphate moieties, one with one acetate on the phosphate group (I) and the other without (II). So to simplify the MS spectra, the acetolyzed products were subsequently peracetylated to obtain predominantly the di-ester species (ions I). The number of acetate groups was verified by deutero-acetolysis followed by perdeutero-acetylation.

Ac_3PIM_2 was treated by acetolysis, and the reaction products were analyzed by ESI-MS in positive and negative modes. As expected, the positive ESI-MS spectrum (Fig. 7*c*) showed an intense peak at m/z 670.9 assigned to ammonium adduct of the di-acylated C_{16}/C_{19} Gro. The negative mass spectrum (Fig. 7*b*) mainly showed one peak at m/z 1284.2 corresponding to the Man_2-Ins-P moiety acylated with one C_{18} arising from the $C_{16}/C_{18}/C_{19}$-PIM_2. Besides this peak, other peaks in lower intensity were observed at m/z 1312.3 and 1326.4 corresponding to Man_2-Ins-P moiety acylated with one C_{16} and one C_{19}, arising from $2C_{16}/C_{19}$- and $C_{16}/2C_{19}$-PIM_2, respectively. Heterogeneity in terms of the nature of the fatty acyl appendage was then observed on the Man*p* unit, but the major population corresponded to C_{16}-Man, as deduced from the intensity of the m/z 1414.2 ions in the ESI source spectrum.

Surprisingly, the parent ion at m/z 1456.2 ($C_{16}/2C_{19}$-PIM_2) gave rise by MS/MS to m/z 745.7 fragment ion identifying the $2C_{19}$-Gro and to the corresponding m/z 803.9 fragment ion identifying the C_{16}-Man_2-Ins-P. This is proof that a Gro bearing $2C_{19}$ exists in minor amounts. Moreover, another ion at m/z 1042.0 was observed corresponding to $2C_{16}$-Man_2-Ins-P

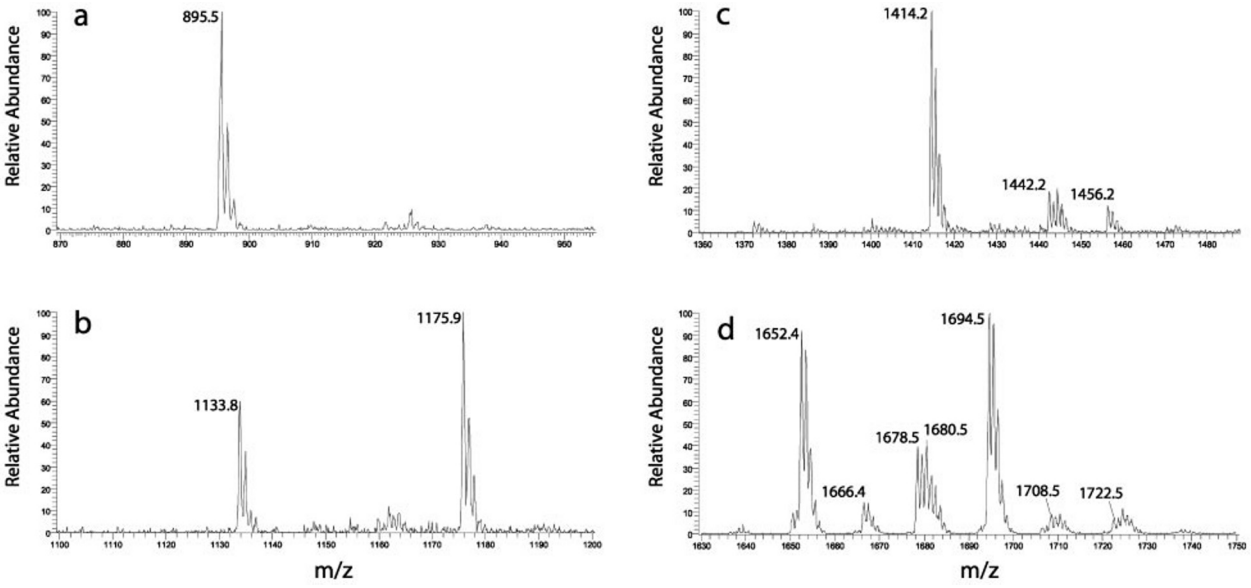

FIG. 4. **Negative ESI mass spectra of the fractions I (*a*), III (*b*), IV (*c*), and V (*d*) of the octyl-Sepharose chromatography.** PIM fatty acyl compositions were based on the most abundant fatty acyl chains found by GC/MS analysis, *i.e.* palmitate (C_{16}), tuberculostearate (C_{19}), and for a lesser extent stearate (C_{18}). Species <2% were not considered. *a,* fraction I corresponds to $C_{16}PIM_2$ (895.5). *b*, fraction III corresponds to Ac_2PIM_2 acylated by C_{16}/C_{16} (1133.8) (38%) and C_{16}/C_{19} (1175.9) (62%). *c,* fraction IV corresponds to Ac_3PIM_2 acylated predominantly by $2C_{16}$,C_{19} (1414.2) (77%) but also by C_{16},C_{18},C_{19} (1442.2) (14%), and C_{16},$2C_{19}$ (1456.2) (9%). *d*, fraction V corresponds to Ac_4PIM_2 acylated predominantly by $3C_{16}$,C_{19} (1652.4) (33%), $2C_{16}$,$2C_{19}$ (1694.5) (36%), $2C_{16}$,$C_{18:1}$,C_{19} (1678.5) (14%), and $2C_{16}$,C_{18},C_{19} (1680.5) (12%) but also by $2C_{16}$,$2C_{18}$ (1666.4) (5%). C_{16},$2C_{18}$,C_{19} (1708.5) and C_{16},C_{18},$2C_{19}$ (1722.5) also exist as minor components.

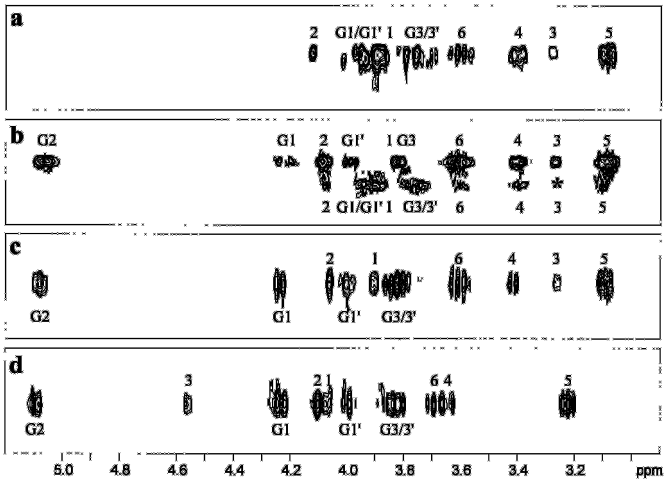

FIG. 5. **^1H-^{31}P HMQC-HOHAHA spectra of Ac_1PIM_2 (*a*), Ac_2PIM_2 (*b*), Ac_3PIM_2 (*c*), and Ac_4PIM_2 (*d*) dissolved in $CDCl_3$/CD_3OD/D_2O 60:35:8 at 303 (*a* and *b*), 305 (*c*), and 293 K (*d*).** *Numerals* correspond to the proton number of the *myo*-Ins unit, and numerals with letter *G* correspond to the proton number of the glycerol unit.

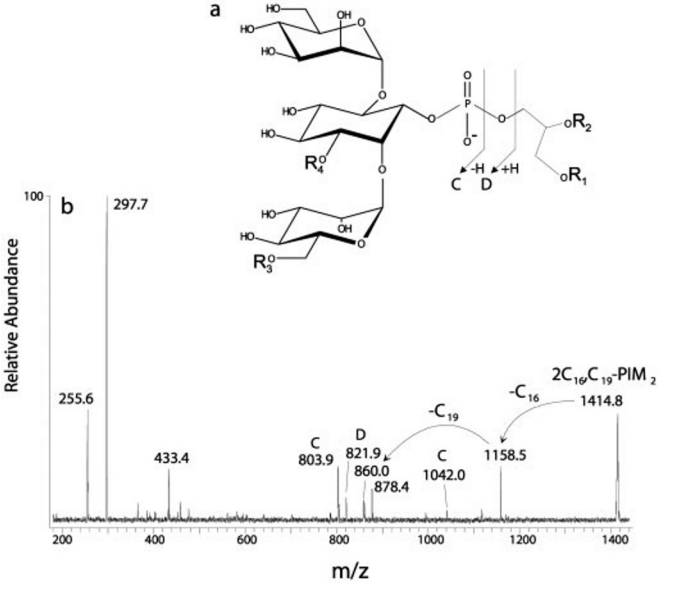

FIG. 6. **Fragmentation scheme (*a*) and negative ESI-MS/MS spectrum of Ac_3PIM_2 ($2C_{16}/C_{19}$) (1414.8) (*b*).** *m*/*z* 255.6, C_{16} carboxylate; *m*/*z* 297.7 C_{19} carboxylate; *m*/*z* 433.4, opening of the phosphate linkage with retention of the glycerol with R_1, R_2 = H, C_{19}; *m*/*z* 803.9, ion C with R_3, R_4 = H, C_{16}; *m*/*z* 821.9, ion D with R_3, R_4 = H, C_{16}; *m*/*z* 860.0, loss of C_{16} and C_{19} in the carboxylic form; *m*/*z* 878.4, loss of C_{16} in the acidic form and C_{19} as a ketene; *m*/*z* 1042.0, ion C with R_3, R_4 = C_{16}, C_{16}; *m*/*z* 1158.5, loss of C_{16}.

and confirming the presence of the lyso-Gro population evidenced by NMR.

Taken together, these results indicate that Ac_3PIM_2 predominantly exists with 2 C_{16} and 1 C_{19}, the glycerol being diacylated by C_{16}/C_{19} and the mannose bearing a C_{16}.

Ac_4PIM_2 Acyl Forms—The negative ESI mass spectrum of fraction V (Fig. 4*d*) showed more peaks than that of the fraction IV (Fig. 4*c*) revealing a higher number of acyl forms. However, all these peaks were in agreement with tetra-acyl forms of PIM_2 (Ac_4PIM_2) and arose from the presence of three types of fatty acids, C_{16}, C_{18}, and C_{19}. Indeed, the most abundant $[M - H]^-$ ions at *m*/*z* 1652.4 (33%), 1680.5 (12%), and 1694.5 (36%) characterized PIM_2 acylated by ($3C_{16}$, $1C_{19}$), ($2C_{16}$, $1C_{18}$, $1C_{19}$), and ($2C_{16}$, $2C_{19}$), respectively. Astonishingly, the signal at *m*/*z* 1678.5 (13%) highlighted a PIM_2 tetra-acylated with $2C_{16}$, $1C_{18:1}$, and $1C_{19}$. Besides these major compounds, another rather abundant species (5%) was observed at *m*/*z* 1666.4 corresponding to PIM_2 acylated with $2C_{16}$ and $2C_{18}$.

The acylation positions were determined previously in an NMR study of Ac_4PIM_2 (12). Three of the fatty acyl residues were localized on both positions of Gro and on the C-3 of the *myo*-Ins unit by two-dimensional ^1H-^{31}P HMQC and HMQC-HOHAHA analysis (Fig. 5*d*). The localization of the fourth fatty acid, on the C-6 of the Man*p,* was deduced from the ^1H-^{13}C HMBC spectrum. As for the Ac_3PIM_2, the acetolysis experi-

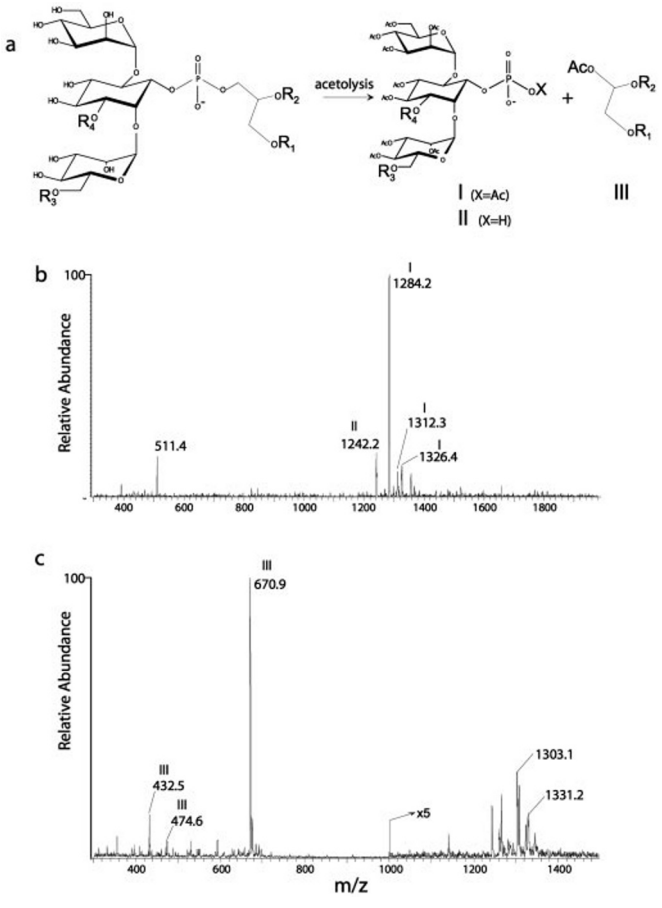

FIG. 7. **Acetolysis reaction (*a*), and negative (*b*), and positive (*c*) ESI mass spectra of Ac_3PIM_2 acetolysis products.** *b,* negative mode: 511.4 $(M - H)^-$ of peracetylated Ins-P contaminant; 1242.2, I as $(M - H)^-$ with $X = H$, $(R_3, R_4) = (C_{16}, Ac)$; 1284.2, I as $(M - H)^-$ with $X = Ac$, $(R_3, R_4) = (C_{16}, Ac)$; 1312.3, I as $(M - H)^-$ with $X = Ac$, $(R_3, R_4) = (C_{18}, Ac)$; 1326.4, I as $(M - H)^-$ with $X = Ac$, $(R_3, R_4) = (C_{19}, Ac)$. *c,* positive mode in presence of ammonium acetate: 432.5, III as $(M + NH_4)^+$ with $(R_1, R_2) = (C_{16}, Ac)$; 474.6, III as $(M + NH_4)^+$ with $(R_1, R_2) = (C_{19}, Ac)$; 670.9, III as $(M + NH_4)^+$ with $(R_1, R_2) = (C_{16}, C_{19})$; 1303.1, I as $(M + NH_4)^+$ with $(R_3, R_4) = (C_{16}, Ac)$; 1331.2, I as $(M + NH_4)^+$ with $(R_3, R_4) = (C_{18}, Ac)$.

ment revealed a Gro mainly acylated by C_{16}/C_{19} ($[M - H]^-$ at m/z 670.8). The C_{16}/C_{16}-Gro and C_{16}/C_{18}-Gro structures, identifiable by $[M - H]^-$ ions at m/z 629.0 and 657.0, respectively, were never observed. The negative mode mass spectrum showed three peaks at m/z 1480.7, 1508.7, and 1522.8 assigned to C_{16}/C_{16}-Man_2-Ins-P, C_{16}/C_{18}-Man_2-Ins-P, and C_{16}/C_{19}-Man_2-Ins-P, respectively. These structures were supported by the ESI-MS/MS spectra from the precursor ions at m/z 1652.4 ($3C_{16}/C_{19}$-PIM_2), m/z 1680.5 ($2C_{16}/C_{18}/C_{19}$-PIM_2), and m/z 1694.5 ($2C_{16}/2C_{19}$-PIM_2) which gave rise to the m/z 1041.2 ($2C_{16}$-Man_2-Ins-P), m/z 1070.3 (C_{16}/C_{18}-Man_2-Ins-P), and m/z 1084.3 (C_{16}/C_{19}-Man_2-Ins-P) fragment ions, respectively.

In order to investigate the relative positions of these fatty acids on the Man_2-Ins-P moiety, peracetylated Ac_4PIM_2 was analyzed by pyrolysis EI/MS. This method results in the cleavage of the interglycosidic linkage leading to oxonium ions (33). Besides the peracetylated mannose oxonium ions at m/z 331.2, only the oxonium fragment at m/z 527.2 (triacetylated mannose with C_{16}) could be detected but not that at m/z 555.2 (triacetylated mannose with C_{18}) nor that at m/z 569.2 (triacetylated mannose with C_{19}). Taken together, these results indicate that the glycerol is always acylated by C_{16}/C_{19} and the mannose by a C_{16}, whereas the nature of the fatty acid present on the inositol is highly variable, being C_{16}, C_{18}, or C_{19}.

The Minor PIM_2 Acyl Forms (Fractions I–III)—When analyzed in ESI-MS, the fraction I spectrum revealed deprotonated molecular ions at m/z 895.5 (Fig. 4*a*), whereas fraction II showed deprotonated molecular ions at m/z 937.5. These ions were assigned to mono-acyl forms of PIM_2 (Ac_1PIM_2), containing C_{16} and C_{19} for fractions I and II, respectively. The ^1H-^{31}P HMQC-HOHAHA (Fig. 5*a*) and HOHAHA (not shown) spectra realized on $C_{19}PIM_2$ revealed that all the Gro protons resonated between 3.7 and 4.0 ppm. The chemical shifts of the *myo*-Ins protons ($\delta_{H\text{-}1}$ 3.89, $\delta_{H\text{-}2}$ 4.10, $\delta_{H\text{-}3}$ 3.28, $\delta_{H\text{-}4}$ 3.39, $\delta_{H\text{-}5}$ 3.09, and $\delta_{H\text{-}6}$ 3.60) indicated that this unit was not acylated. A more accurate definition of the $C_{16}PIM_2$ Gro spin system by ^1H-^{13}C HMQC experiment led to the definition of H-1 at δ 3.90/3.94 and H-3 at δ 3.70/3.75. These chemical shifts were in agreement with an acylation of position 1 by comparison with Gro chemical shifts of the standard L-α-lysophosphatidylinositol in Me_2SO-d_6 (1-acyl-2-lyso-*sn*-glycero-3-phospho-(1-D-*myo*-Ins): $\delta_{H\text{-}1/H\text{-}1'}$ 3.99/3.97; $\delta_{H\text{-}2}$ 3.75; $\delta_{H\text{-}3/H\text{-}3'}$ 3.78/3.76) and the standard 1-oleyl-2-lysophosphatidic acid in chloroform/methanol/water ($\delta_{H\text{-}1/H\text{-}1'}$ 4.05/4.11; $\delta_{H\text{-}2}$ 3.95; $\delta_{H\text{-}3/H\text{-}3'}$ 3.83/3.89). Moreover, the $\delta_{C\text{-}6}$ of Man at 62.7 ppm and the $\delta_{H\text{-}6}$ between 3.47 and 3.64 ppm excluded acylation on this position. Thus, it can be proposed that mono-acyl forms of PIM_2 are acylated on the Gro at the C-1 position whatever the nature of the fatty acid (C_{16} or C_{19}). This conclusion is in agreement with ESI-MS/MS experiments and ESI-MS analysis of the acetolysis products of Ac_1PIM_2. Indeed, the Man_2-Ins-P moiety of Ac_1PIM_2 was found devoid of fatty acids (ions at m/z 565.4/583.4 and 1087.8, respectively). Concerning the Gro part, fragment ions corresponding to C_{19}-Gro (at m/z 433.5/451.6) were obtained from the m/z 937.5 parent ion ($C_{19}PIM_2$). The analogous fragments corresponding to C_{16}-Gro (at m/z 391.5/409.5) expected from the m/z 895.5 parent ions ($C_{16}PIM_2$) were not observed. However, the acetolysis experiment unambiguously evidenced C_{16}-Gro ($[M + NH_4]^+$ at m/z 432.6) and C_{19}-Gro ($[M + NH_4]^+$ at m/z 474.7).

The ESI mass spectrum corresponding to fraction III showed two peaks at m/z 1133.8 and 1175.9 (Fig. 4*b*) assigned to deprotonated molecular ions of di-acyl forms of PIM_2 (Ac_2PIM_2). They characterized $(M - H)^-$ ions of PIM_2 acylated by $2C_{16}$ (m/z 1133.8 (38%)), $1C_{16}$, and $1C_{19}$ (m/z 1175.9 (62%)). The acylation positions were investigated by NMR analysis. The ^1H-^{31}P HMQC-HOHAHA spectra (Fig. 5*b*) clearly showed two lines of correlations, highlighting two distinct populations of Ac_2PIM_2. The most representative one (80%, determined from the ^{31}P signal height) corresponded to a population bearing fatty acids on both positions of Gro since the H-2 was deshielded at 5.06 ppm (Fig. 5*b*). The Gro proton chemical shifts of the other population were similar to those described for Ac_1PIM_2 since all the Gro protons resonated between 3.7 and 4.0 ppm. These chemical shifts were in agreement with acylation of Gro at position 1. Moreover, as the *myo*-Ins proton chemical shifts were also similar to those described in the case of Ac_1PIM_2, we assumed that *myo*-Ins was not acylated and, by deduction, that Man*p* was acylated in position 6. The existence of these two populations is perhaps more obvious from the ^1H-^{13}C HMQC analysis, where the two sets of correlations, *i.e.* those corresponding to the di-acyl Gro and those corresponding to the lyso-Gro, were clearly observed as two different phosphorus resonances (not shown). The two populations of Ac_2PIM_2, evidenced by NMR, were confirmed by MS/MS data. Indeed, beside the ions corresponding to a non-acylated Man_2-Ins-P moiety (m/z 565.4), ions arising from C_{16}-Man_2-Ins-P (m/z 803.9/821.9) were observed from the parent ions at m/z 1133.8 ($2C_{16}$) and m/z 1175.9 (C_{16}/C_{19}) parent ions. Similarly, in addition to the non-acylated Man_2-Ins-P (at m/z 1087.8), the

TABLE I
Major PI and PIM_2 acyl forms evidenced in M. bovis BCG
The relative abundance of the different species for each acyl form was determined from the integration of the corresponding monoisotopic signals.

Ac_2PI	C_{16}, C_{19}	Gro		Man*p*, 6	*myo*-Ins, 3	Abundance
		1	2			
		C_{16}	C_{19}			
Ac_1PIM_2	C_{16}	C_{16}				
	C_{19}	C_{19}				
Ac_2PIM_2	C_{16}, C_{19}	C_{16}	C_{19}			62%
	C_{16}, C_{16}	C_{16}	C_{16}			38%
Ac_3PIM_2	$2C_{16}$, C_{19}	C_{16}	C_{19}	C_{16}		77%
	C_{16}, C_{18}, C_{19}	C_{16}	C_{19}	C_{18}		14%
	C_{16}, $2C_{19}$	C_{16}	C_{19}	C_{19}		9%
Ac_4PIM_2	$3C_{16}$, C_{19}	C_{16}	C_{19}	C_{16}	C_{16}	42%
	$2C_{16}$, $2C_{19}$	C_{16}	C_{19}	C_{16}	C_{19}	38%
	$2C_{16}$, C_{18}, C_{19}	C_{16}	C_{19}	C_{16}	C_{18}	14%

acetolysis experiment evidenced a weak signal at m/z 1284.2 corresponding to C_{16}-Man_2-Ins-P.

The question is now to localize the fatty acids on both positions of the glycerol. Working on phosphatidylinositol, it was noted by Hsu and Turk (34) that loss of fatty acid at the *sn*-2 position occurs more favorably than that at *sn*-1 by MS-MS of deprotonated molecular ions. The ESI-MS/MS spectrum of C_{16}/C_{19}-PIM_2 (at m/z 1175.9) showed fragment ions at m/z 877.4 (-C_{19}) which appeared more intense than the ones at 919.5 (-C_{16}), leading to the conclusion that C_{19} is present at the *sn*-2 position and C_{16} at *sn*-1 (Table I).

Recruitment of CD1d-restricted NK T Cells in the Granulomatous Lesions Generated by PIM and PI Acyl Forms—As mentioned previously, fractions containing PIM_2 and PIM_6 generated similar lesions with no obvious difference in size revealing that the degree of mannosylation plays no role. To examine the specificity of PIM_2 to recruit NK T cells in the granulomatous lesions, the purified PIM_2 acyl forms described previously were tested. In addition, the cell infiltrates or granuloma were assayed for the presence of CD1d1-restricted T cells identified by the presence of the invariant Vα14-Jα281 TCR α chain. PBS-Alum, used as a negative control and which induced only a minor infiltration (Fig. 8) was found negative for both the infiltration of total Vα14$^+$ T cells (Fig. 8, *left panel*) and that of Vα14-J281$^+$ (*i.e.* CD1d1-restricted T cells) (Fig. 8, *right panel*). The fully deacylated PIM_2 generated identical signals thus extending to the recruitment of NK T cells, the absolute dependence of the response upon the presence of fatty acid chains. By contrast, PI with two acid chains as well as PIM_2 with one to four acyl chains, in addition to generating a granulomatous response, also induced the local infiltration of the lesions by NK T cells (Fig. 8, *right panels*). Moreover, the infiltration by NK T cells was nearly exclusive since no other Vα14$^+$ T cells were recovered in the lesions, excluding random infiltration of lymphocytes that should have mimicked the Vα14 profile of total spleen or liver T cells (Fig. 8, *bottom panels*). The data obtained by using PCR at saturation were only semi-quantitative but, for an identical HPRT mRNA content, suggested an equivalent number of Vα14-Jα281 mRNA chains in all positive samples. Thus, the number of fatty acid chains does not interfere with the recruitment of NK T cells, and the recruitment of the latter cells by PI of mycobacterial origin strengthened the hypothesis according to which the carbohydrate moiety played only a minor role in the biological response.

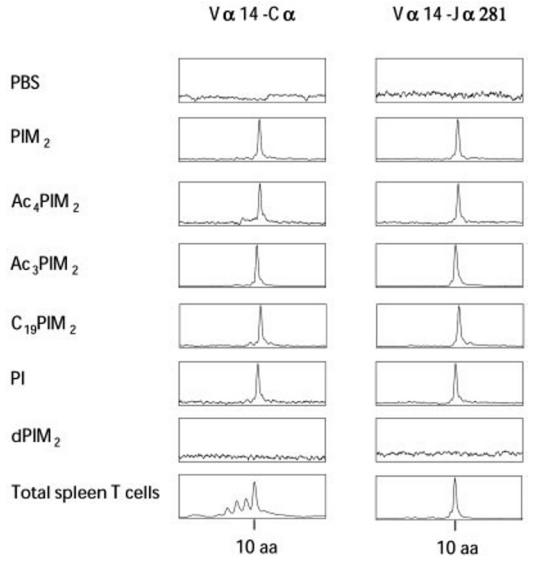

FIG. 8. **Immunoscope profiles of the Vα14 rearranged TCR α chains in cell infiltrates.** Cell infiltrates were collected on day 7 following the injection. The molecules injected are shown on the *left* of the figure. *Left panels*, Vα14-Cα rearrangements, and *right panels*, Vα14-Jα281 rearrangements. *Ordinate*, relative scale of fluorescence intensity. *Abscissa*, size of the CDR3 region in amino acids.

DISCUSSION

The results presented herein solve several questions left in abeyance for many years concerning the structural definition of the phosphatidylinositol-mannosides. Although their mannooligosaccharidic part is perfectly defined (5), a blur existed concerning the acylated state of these molecules. This point is plainly of great importance as the metabolic control of the acylation state may be involved in the fine-tuning of their biological activities. For a structural elucidation of the different populations existing, purification is a crucial step. We developed a rapid and effective method allowing the retrieval of purified acyl forms in three steps as follows: (i) lipidic extraction and phospholipidic precipitation, (ii) QMA column to discriminate neutral from charged molecules and PIM_2 from PIM_6, and (iii) octyl-Sepharose column on PIM_2 or PIM_6 mixtures to separate acyl forms. PIM were predominantly found in the chloroform/methanol extract. Despite our efforts to purify them from the ethanol/water extract, very little was retrieved.

The heterogeneous nature of these closely related molecules defies their purification to homogeneity using isocratic silicic flash chromatography. Ac_4PIM_2 could be easily purified in this way (12) as it is very apolar, but this strategy was unsuccessfully applied to purify the more polar PIM_2, as they co-migrate with the more acylated forms of PIM_6. The strategy described here allowed us first to separate PIM_2 from PIM_6 and second to

fractionate them according to their acylation degree.

M. bovis BCG and M. smegmatis strain 607[3] were found to mainly contain two PIM families, the dimannoside (PIM_2) and the hexamannoside (PIM_6). PIM_1, PIM_3, PIM_4, and PIM_5 were observed in very small quantities, suggesting that they are biosynthetic intermediates. For each glyco form, tri- and tetra-acylated molecules were the most abundant.

The structural strategy used to characterize acylation sites combines the potential of two complementary analytical techniques, NMR and mass spectrometry. NMR has the advantage of taking into account the globality of the fraction but the sensitivity is less than that of mass spectrometry. Electrospray ionization mode was chosen rather than FAB as the molecules could be analyzed without derivatization preventing the loss of any labile substituents. Classical chemical procedures as protection of free hydroxyls by base-stable *O*-(1-methoxy)-ethylated groups after reaction with methyl vinyl ether, where only acylation sites are revealed as *O*-methylated sugars by GC/MS analysis (35) or Prehm methylation followed by FAB-MS analysis as described by Khoo *et al.* (11), could help answering this question. They were discarded as they imply several chemical steps and as they require higher amounts of sample than ESI mass spectrometry. Moreover, in our strategy, NMR was used to characterize the acylation positions, and mass spectrometry gave information concerning the nature of the fatty acids present at each position. The results obtained are summarized in Table I. Ac_1PIM_2 is identified with C_{16} or C_{19} in position 1 of the Gro. Ac_2PIM_2 appears as two populations equally represented, one with 2 C_{16} and one with 1 C_{16} and 1 C_{19}, both fatty acids being on Gro. These data contrast with those of Brennan and co-workers (11) who demonstrated that the Ac_2PIM_2 exists predominantly as lyso-PIM_2. Concerning Ac_3PIM_2, a major acyl form was observed, corresponding to PIM_2 with 2 C_{16} and 1 C_{19}, the glycerol being di-acylated by C_{16}/C_{19} and the mannose bearing a C_{16}. Interestingly, the acyl form corresponding to $3C_{16}$-PIM_2 was not observed, indicating that Ac_3PIM_2 arose from C_{16}/C_{19}-PIM_2. Ac_4PIM_2 was present as three populations: $3C_{16}/C_{19}$-, $2C_{16}/2C_{19}$-, and $2C_{16}/C_{18}/C_{19}$-PIM_2. The acylation positions were clearly elucidated in an earlier NMR study (12) as being both positions of Gro, the C-3 of the *myo*-Ins unit and the C-6 of the Man*p* linked to the C-2 of the *myo*-Ins unit, excluding the presence of a fatty acid to the C-6 of the Man*p* linked on the C-6 of the *myo*-Ins unit envisaged by Khoo *et al.* (11). Taken together, the results indicate that the glycerol is preferentially acylated by C_{16}/C_{19}, the mannose by one C_{16}, even if a weak variation exits. However, the nature of the fatty acid present on the inositol appears highly variable being C_{16}, C_{18}, or C_{19}.

These results have led to advances in answering the question whether PIM are biosynthetic precursors of LM and LAM or not. The definition of the acyl forms of LAM and LM was approached by an NMR strategy applied on the native molecules (12, 36, 37). Indeed, the one-dimensional ^{31}P NMR spectra of LAM and LM from *M. bovis* BCG typify the anchor heterogeneity and lead to the characterization of at least five populations of differently acylated molecules. Then two-dimensional ^{1}H-^{31}P NMR spectroscopy allowed the definition of mono- to at least tri-acylated molecules. In the case of LAM and LM, NMR was unable to confirm the highly suspected presence of fatty acid on the C-6 of the Man*p* due to the larger number of mannose units. Nevertheless, the purification of each population followed by matrix-assisted laser desorption ionization/time of flight-mass spectrometric analyses allowed the unambiguous characterization of the tetra-acyl form, in addition to the mono- to tri-acyl forms.[3] Taken together, the results highlight the same major fatty acids and acylation sites for all these molecules strongly suggesting a biosynthetic filiation between them.

PIM, independently of their glyco forms and acyl forms, have the capacity to recruit NK T cells in the granulomatous region. From our results, two main conclusions can be reached concerning the structural requirement of such activity. First, to generate a granulomatous response and to recruit NK T cells, there is an absolute requirement for the molecules to possess at least one fatty acyl chain, with no evidence for differences related to their number, location, or size. Second, the increasing complexity of the carbohydrate moiety is not reflected in significant differences in the biological responses. In this respect, it is worth noting that mycobacterial PI behaved primarily like PIM_2 and PIM_6, a finding indicative of the minor role of the carbohydrates in NK T cell recruitment as well as a lack of specificity of the TCR of NK T cells toward sugars as suggested independently by analysis of the TCR repertoire (21, 38) and the use of CD1d1 tetramers (39).

The Vα14$^+$ invariant TCR α chain typifies CD1d-restricted NK T cells that are activated by exogenous antigens such as α-GalCer. This TCR of CD1d-restricted NK T cells is highly discriminating for α-GalCer analogs. Indeed, discrete structural modification of the α-GalCer carbohydrate part either by adding an extra α-Gal or by changing the α-anomer into a β-anomer or by epimerization of the hydroxyl group at position 2 of α-GalCer led to non-activation of CD1d-restricted NK T cells (40–42). In contrast to these results, our data reveal that PI, which does not contain carbohydrate, presents the same ability as PIM_2 or PIM_6 to recruit Vα14-invariant NK T cells preferentially to other rearranged Vα14$^+$ T cells, which are undetectable in the granuloma. This suggested the absence of a TCR-specific recognition by the TCR of NK T cells and consequently the absence of role of the TCR-CD1 axis in NK T cell recruitment.

In addition, Ac_3- and Ac_4PIM_2 show the same activity as Ac_1PIM_2 and Ac_2PIM_2. To date, the glycolipids loaded by CD1b molecules have two aliphatic chains (43). This is also the case for the exogenous antigen α-GalCer presented by CD1d. This is consistent with the fact that CD1d is composed of a hydrophobic antigen-presenting groove with two large pockets that probably accommodate two acyl appendages (44). In the case of PIM, the extra acyl appendages located on Man*p* and/or on *myo*-Ins could prevent tri- and tetra-acylated PIM recognition by the TCR of NK T cells again supporting the idea that recruitment of Vα14 invariant NK T cells is not controlled by the TCR-CD1d axis. This hypothesis is in agreement with adoptive transfer experiments of wild type NK T cells into CD1d1$-/-$ mice showing that CD1d1 expression is not required for the early recruitment of NK T cells to the injection site.[4] Taken together, these data strongly suggest that the TCR-CD1d axis is not important for the NK T cell activation and recruitment to the injection site. These data rather fit with NK T cells being attracted to the site of inflammation caused by glycolipids, irrespective of their carbohydrate and fatty acyl moieties.

It should be kept in mind that the present bioassay does not reflect only early events in the recognition of glycolipids but rather the result of complex and sequential cell-to-cell interactions due to the occurrence of foreign glycolipids. The rationale for the use of the present bioassay is based on the inability to activate NK T cells *in vitro* using reagents other than α-galac-

[3] M. Gilleron and G. Puzo, unpublished results.

[4] M. Mempel, C. Ronet, F. Suasez, M. Gilleron, G. Puzo, Y. Koezuko, L. van Kaes, A. Lehuen, P. Kourilsky, and G. Gachelin, manuscript submitted for publication.

tosylceramide (41) or anti-CD3 monoclonal antibodies (45). This precludes the monitoring of the early release of interferon-γ and interleukin-4 (46) that could occur following encounters with foreign ligands. The need for such an assay aimed at deciphering early events following glycolipid recognition is stressed by the finding that PIM recruit NK T cells without inducing their apoptosis (data not shown), whereas NK T cells are involved in a variety of immune processes ranging from the keeping of pregnancy to anti-cancer responses (47).

REFERENCES

1. Ballou, C. E., Vilkas, E., and Lederer, E. (1963) *J. Biol. Chem.* **238,** 69–76
2. Lee, Y. C., and Ballou, C. E. (1964) *J. Biol. Chem.* **239,** 1316–1327
3. Lee, Y. C., and Ballou, C. E. (1965) *Biochemistry* **4,** 1395–1404
4. Chatterjee, D., Hunter, S. W., McNeil, M., and Brennan, P. J. (1992) *J. Biol. Chem.* **267,** 6228–6233
5. Severn, W. B., Furneaux, R. H., Falshaw, R., and Atkinson, P. H. (1998) *Carbohydr. Res.* **308,** 397–408
6. Nojima, S. (1959) *J. Biochem.* (*Tokyo*) **46,** 607–620
7. Pangborn, M. C., and McKinney, J. A. (1966) *J. Lipid Res.* **7,** 627–633
8. Brennan, P., and Ballou, C. E. (1967) *J. Biol. Chem.* **242,** 3046–3056
9. Khuller, G. K., and Subrahmanyam, D. (1968) *Experentia* (*Basel*) **24,** 851–852
10. Leopold, K., and Fischer, W. (1993) *Anal. Biochem.* **208,** 57–64
11. Khoo, K. H., Dell, A., Morris, H. R., Brennan, P. J., and Chatterjee, D. (1995) *Glycobiology* **5,** 117–127
12. Gilleron, M., Nigou, J., Cahuzac, B., and Puzo, G. (1999) *J. Mol. Biol.* **285,** 2147–2160
13. Chatterjee, D., and Khoo, K. H. (1998) *Glycobiology* **8,** 113–120
14. Vercellone, A., Nigou, J., and Puzo, G. (1998) *Front. Biosci.* **3,** 149–163
15. Gilleron, M., Riviere, M., and Puzo, G. (2001) in *Glycans in Cell Interaction and Recognition: Therapeutic Aspects* (Aubery, M., ed), pp. 113–140, Harwood Academic Publishers GmbH, Amsterdam
16. Sieling, P. A., Chatterjee, D., Porcelli, S. A., Prigozy, T. I., Mazzaccaro, R. J., Soriano, T., Bloom, B. R., Brenner, M. B., Kronenberg, M., Brennan, P. J., and Modlin, R. L. (1995) *Science* **269,** 227–230
17. Ernst, W. A., Maher, J., Cho, S., Niazi, K. R., Chatterjee, D., Moody, D. B., Besra, G. S., Watanabe, Y., Jensen, P. E., Porcelli, S. A., Kronenberg, M., and Modlin, R. L. (1998) *Immunity* **8,** 331–340
18. Porcelli, S. A., Segelke, B. W., Sugita, M., Wilson, I. A., and Brenner, M. B. (1998) *Immunol. Today* **19,** 362–368
19. Lantz, O., and Bendelac, A. (1994) *J. Exp. Med.* **180,** 1097–1106
20. Apostolou, I., Takahama, Y., Belmant, C., Kawano, T., Huerre, M., Marchal, G., Cui, J., Taniguchi, M., Nakauchi, H., Fournie, J. J., Kourilsky, P., and Gachelin, G. (1999) *Proc. Natl. Acad. Sci. U. S. A.* **96,** 5141–5146
21. Ronet, C., Mempel, M., Thieblemont, N., Lehuen, A., Kourilsky, P., and Gachelin, G. (2001) *J. Immunol.* **166,** 1755–1762
22. Zeng, Z.-H., Castano, A. R., Segelke, B. W., Stura, E. A., Peterson, P. A., and Wilson, I. A. (1997) *Science* **277,** 339–345
23. Joyce, S., Woods, A. S., Yewdell, J. W., Bennink, J. R., De Silva, A. D., Boesteanu, A., Balk, S. P., Cotter, R. J., and Brutkiewicz, R. R. (1998) *Science* **279,** 1541–1544
24. Vercellone, A., and Puzo, G. (1989) *J. Biol. Chem.* **264,** 7447–7454
25. Marion, D., and Wuthrich, K. (1983) *Biochem. Biophys. Res. Commun.* **113,** 967–974
26. Bax, A., and Davis, D. G. (1985) *J. Magn. Reson.* **65,** 355–360
27. Bax, A., and Subramanian, S. (1986) *J. Magn. Reson.* **67,** 565–569
28. Shaka, A. J., Barker, P. B., and Freeman, R. (1985) *J. Magn. Reson* **64,** 547–552
29. Bax, A., and Summers, M. F. (1986) *J. Am. Chem. Soc.* **108,** 2093–2094
30. Lerner, L., and Bax, A. (1986) *J. Magn. Reson.* **69,** 375–380
31. Gilleron, M., Vercauteren, J., and Puzo, G. (1993) *J. Biol. Chem.* **268,** 3168–3179
32. Wang, Y., and Hollingsworth, R. I. (1995) *Anal. Biochem.* **225,** 242–251
33. Fournie, J. J., Riviere, M., and Puzo, G. (1987) *J. Biol. Chem.* **262,** 3174–3179
34. Hsu, F. F., and Turk, J. (2000) *J. Am. Soc. Mass Spectrom.* **11,** 986–999
35. De Belder, A. N., and Normann, B. (1968) *Carbohydr. Res.* **8,** 1–6
36. Nigou, J., Gilleron, M., and Puzo, G. (1999) *Biochem. J.* **337,** 453–460
37. Gilleron, M., Bala, L., Brando, T., Vercellone, A., and Puzo, G. (2000) *J. Biol. Chem.* **275,** 677–684
38. Apostolou, I., Cumano, A., Gachelin, G., and Kourilsky, P. (2000) *J. Immunol.* **165,** 2481–2490
39. Benlagha, K., Weiss, A., Beavis, A., Teyton, L., and Bendelac, A. (2000) *J. Exp. Med.* **191,** 1895–1903
40. Prigozy, T. I., Naidenko, O., Qasba, P., Elewaut, D., Brossay, L., Khurana, A., Natori, T., Koezuka, Y., Kulkarni, A., and Kronenberg, M. (2001) *Science* **291,** 664–667
41. Kawano, T., Cui, J., Koezuka, Y., Toura, I., Kaneko, Y., Motoki, K., Ueno, H., Nakagawa, R., Sato, H., Kondo, E., Koseki, H., and Taniguchi, M. (1997) *Science* **278,** 1626–1629
42. Brossay, L., Naidenko, O., Burdin, N., Matsuda, J., Sakai, T., and Kronenberg, M. (1998) *J. Immunol.* **161,** 5124–5128
43. Shamshiev, A., Donda, A., Prigozy, T. I., Mori, L., Chigorno, V., Benedict, C. A., Kappos, L., Sonnino, S., Kronenberg, M., and De Libero, G. (2000) *Immunity* **13,** 255–264
44. Matsuda, J. L., and Kronenberg, M. (2001) *Curr. Opin. Immunol.* **13,** 19–25
45. Yoshimoto, T., and Paul, W. E. (1994) *J. Exp. Med.* **179,** 1285–1295
46. Chen, H., and Paul, W. E. (1997) *J. Immunol.* **159,** 2240–2249
47. Godfrey, D. I., Hammond, K. J., Poulton, L. D., Smyth, M. J., and Baxter, A. G. (2000) *Immunol. Today* **21,** 573–583